American Journal of Mathematics and Statistics 2013, 3(4): 179-189
DOI: 10.5923/j.ajms.20130304.01

Comparative Study of Parallel Plate Slider Bearing with Other Slider Bearings Using Magnetic Fluid as Lubricant

Rajesh C. Shah[1,*], M. M. Parsania[2]

[1]Department of Applied Mathematics, Faculty of Technology and Engineering, The M. S. University of Baroda, Vadodara – 390 001, Gujarat State, India
[2]Department of Mathematics, School of Engineering, R.K. University, Rajkot, Gujarat State, India

Abstract The aim of the present paper is to make a comparative study of magnetic fluid lubricated various designed slider bearings (that is, slider bearings having inclined pad stator, exponential pad stator, secant pad stator, convex pad stator) with that of slider bearing having parallel pad stator including effects of porosity, slip velocity at both the ends and squeeze velocity (which appear when the upper plate approach to lower one) under the magnetic field oblique to the lower plate (pad or surface). The paper also studied about the cases of anisotropic permeability and isotropic permeability with respect to both upper and lower porous matrix (layer). The dimensionless load carrying capacity for porous matrixes of various sizes attached at upper and lower plates is calculated for various slider bearings and compared with slider bearing having parallel pad stator. From the results and discussion, it is suggested to have slider bearing design with inclined or convex pad stator surfaces and occasionally secant pad stator surface.

Keywords Magnetic Fluid, Porosity, Slider Bearings, Permeability

1. Introduction

Magnetic fluid or Ferrofluid[1] are stable colloidal suspensions containing fine ferromagnetic particles dispersing in a liquid, called carrier liquid, in which a surfactant is added to generate a coating layer preventing the flocculation of the particles. When an external magnetic field is applied, magnetic fluids experience magnetic body forces depends upon the magnetization of ferromagnetic particles. Owing to these features magnetic fluids are useful in many applications like sensors, centrifugal switches, dampers, etc.[2].

With the advent of magnetic fluid, many authors have worked on magnetic fluid lubrication from different viewpoints, of which some references are as follows:

Tipei[3] studied on theory of lubrication with ferrofluids and applied it to short bearings. Agrawal[4] studied magnetic fluid effects on a porous inclined bearing and found that the magnetization of the magnetic particles in the lubricant increased its load capacity without affecting the friction on the moving slider. Sinha *et. al.*[5] studied ferrofluid lubrication of cylindrical rollers with cavitations. Ram and Verma[6] studied on ferrofluid lubrication in porous inclined slider bearing. Shah and Bhat in[7,8] studied respectively on ferrofluid lubrication of porous slider bearing with velocity slip, and ferrofluid squeeze film between curved annular plates including rotation of magnetic particles. Ahmad and Singh[9] studied on magnetic fluid lubrication of porous-pivoted slider bearing with slip velocity. Recently, Shah and Patel[10] studied on mathematical Modeling of newly designed ferrofluid based slider bearing including effects of porosity, anisotropic permeability, slip velocity at both the ends, and squeeze velocity.

With the motivation that, the porous layer in the bearing is considered because of its advantageous property of self lubrication, the present paper presents comparative study of magnetic fluid lubricated various designed slider bearings (that is, slider bearings having inclined pad stator, exponential pad stator, secant pad stator, convex pad stator) with that of slider bearing having parallel pad stator including effects of porosity, slip velocity at both the ends and squeeze velocity (which appear when the upper plate approach to lower one) under the magnetic field oblique to the lower plate.

A magnetic fluid lubrication equation is derived for the above problem in general and the various sizes of porous matrix are attached to upper and lower plates considered for computation of dimensionless load carrying capacity. Also, it is computed for two different cases of anisotropic permeability and isotropic permeability with respect to both upper and lower porous matrix.

The magnetic fluid flow model considered here is due to R. E. Rosensweig[1] and magnetic fluids used in the

* Corresponding author:
dr_rcshah@yahoo.com (Rajesh C. Shah)
Published online at http://journal.sapub.org/ajms

computations are of water based.

2. Derivation of the Mathematical Model

Figure 1-5 shows schematic diagram of various system of slider bearings under study which consists of a magnetic fluid film of thickness h within a stator pad surface of various shapes and a slider of length A in the x-direction and width B in y-direction, $A << B$. The value of h is h_2 at the inlet and h_1 at the outlet. The expression for film thicknesses h are shown against their bearing design as follows:

(a) For slider bearing having inclined pad stator:

$$h_i = h_2 - (h_2 - h_1)\, x / A \,;\; 0 \le x \le A \qquad (1)$$

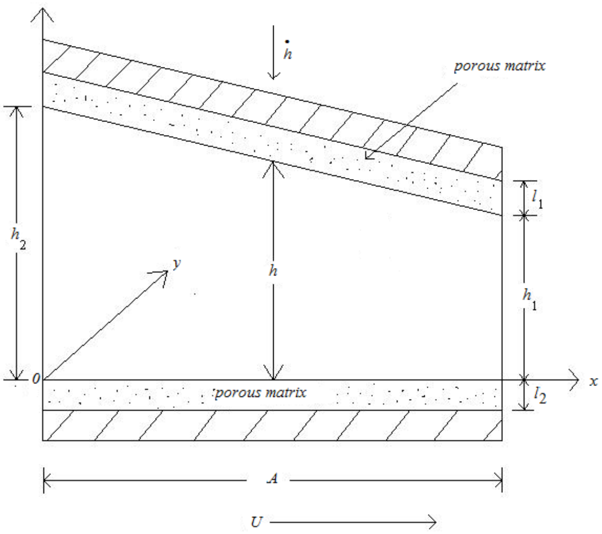

Figure 1. Slider bearing having inclined pad stator

(b) For slider bearing having exponential pad stator:

$$h_e = h_2 e^{-\frac{(x \ln a)}{A}} \;;\; 0 \le x \le A \qquad (2)$$

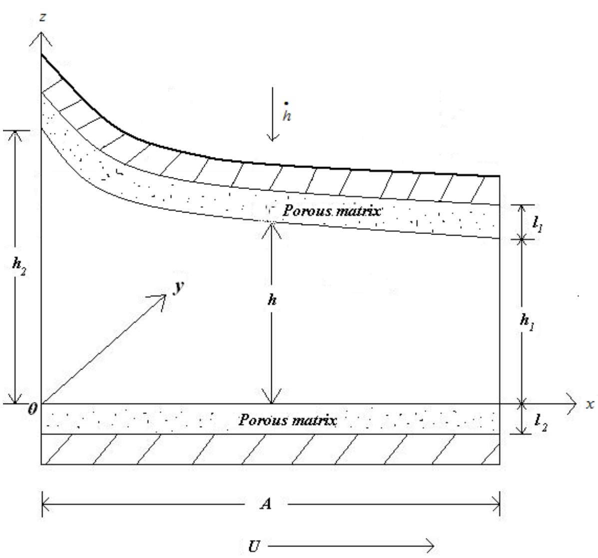

Figure 2. Slider bearing having exponential pad stator

(c) For slider bearing having secant pad stator:

$$h_s = h_1 \sec\left\{\frac{\pi(A-x)}{2A}\right\};\; 0 < x \le A \qquad (3)$$

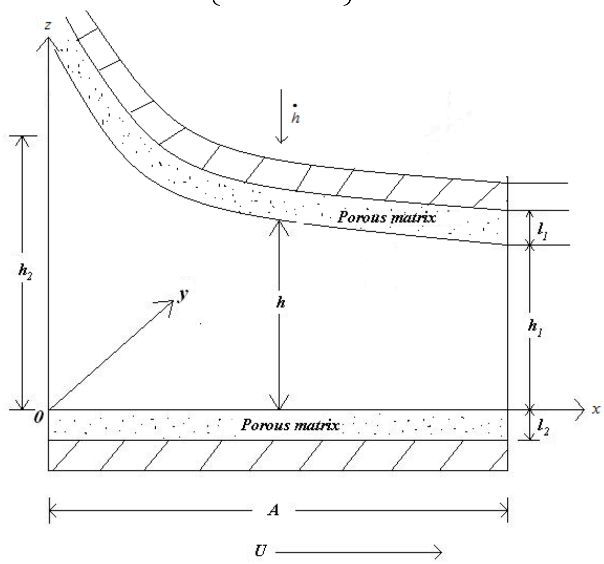

Figure 3. Slider bearing having secant pad stator

(d) For slider bearing having convex pad stator:

$$h_c = 4\delta\left(\frac{x^2}{A^2} - \frac{x}{A}\right) + h_2 - (h_2 - h_1)\frac{x}{A} \;;\; 0 \le x \le A \qquad (4)$$

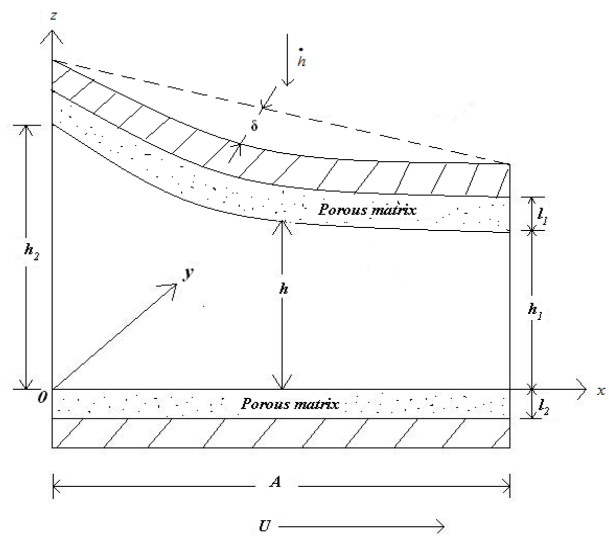

Figure 4. Slider bearing having convex pad stator

where δ is the central thickness of the convex pad.

(e) For slider bearing having parallel pad stator:

$$h_p = h_1 = h_2 \;;\; 0 \le x \le A \qquad (5)$$

Porous matrix of thickness l_2 and l_1 *metres* have attached with the slider and stator respectively. Both the porous matrix are backed by a solid wall. The slider moves with a uniform velocity U in the x-direction. Also, stator moves normally towards the slider with a uniform velocity (known as squeeze velocity) $\dot{h} = dh/dt$, where t is time in *seconds*.

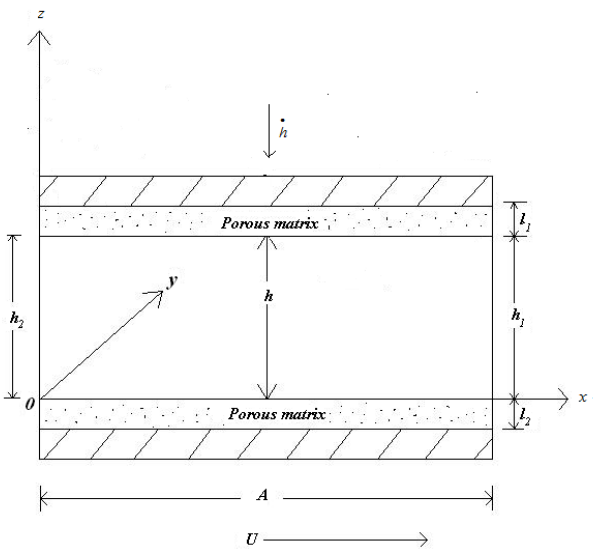

Figure 5. Slider bearing having parallel pad stator

(1) Following[10,11] , the basic equations governing the magnetic fluid flow based on R. E. Rosensweig model are given as follows:

$$\rho\left[\frac{\partial \mathbf{q}}{\partial t}+(\mathbf{q}\bullet\nabla)\mathbf{q}\right]=-\nabla p+\eta\nabla^2\mathbf{q}+\mu_0(\mathbf{M}\bullet\nabla)\mathbf{H} \quad (6)$$

$$\nabla\bullet\mathbf{q}=0 \quad (7)$$

$$\nabla\times\mathbf{H}=0 \quad (8)$$

$$\mathbf{M}=\bar{\mu}\,\mathbf{H} \quad (9)$$

$$\nabla\bullet(\mathbf{H}+\mathbf{M})=0, \quad (10)$$

where ρ, p, η, $\mathbf{q}$, μ_0, $\mathbf{M}$, $\mathbf{H}$, $\bar{\mu}$ are density, film pressure, fluid viscosity, fluid velocity, free space permeability, the magnetization vector, magnetic field vector and magnetic susceptibility respectively.

By combining above equations (6) to (10) under the usual assumption of lubrication, neglecting inertia terms and that the derivatives of velocities across the film predominate, one - dimensional equation governing the lubricant flow in the film region yields

$$\frac{\partial^2 u}{\partial z^2}=\frac{1}{\eta}\frac{\partial}{\partial x}\left(p-\frac{1}{2}\mu_0\bar{\mu}H^2\right), \quad (11)$$

where u is the film fluid velocity in the x-direction and H is the magnetic field strength.

(2)The integral form of continuity equation in the film region is given by

$$\frac{\partial}{\partial x}\int_0^h u\,dz+w_h-w_0=0, \quad (12)$$

where w is the axial component of the fluid velocity in the film.

(3) Using Darcy's law, the velocity components of the fluid in the porous matrix are given as follow:

For upper porous region:

$$\bar{u}_1=-\frac{\psi_x}{\eta}\frac{\partial}{\partial x}\left(P-\frac{1}{2}\mu_0\bar{\mu}H^2\right),\ (x-\text{direction}) \quad (13)$$

$$\bar{w}_1=-\frac{\psi_z}{\eta}\frac{\partial}{\partial z}\left(P-\frac{1}{2}\mu_0\bar{\mu}H^2\right),\ (z-\text{direction}) \quad (14)$$

where ψ_x,ψ_z are fluid permeabilities in the upper porous region in x and z directions respectively, and P is the fluid pressure in the porous region.

For lower porous region:

$$\bar{u}_2=-\frac{\varphi_x}{\eta}\frac{\partial}{\partial x}\left(P-\frac{1}{2}\mu_0\bar{\mu}H^2\right),\ (x-\text{direction}) \quad (15)$$

$$\bar{w}_2=-\frac{\varphi_z}{\eta}\frac{\partial}{\partial z}\left(P-\frac{1}{2}\mu_0\bar{\mu}H^2\right),\ (z-\text{direction}) \quad (16)$$

where φ_x,φ_z are fluid permeabilities in the lower porous region in x and z directions respectively, and P is the fluid pressure in the porous region.

(4)The continuity equation in the porous regions are given as follows:

For upper porous region:

$$\frac{\partial\bar{u}_1}{\partial x}+\frac{\partial\bar{w}_1}{\partial z}=0. \quad (17)$$

For lower porous region:

$$\frac{\partial\bar{u}_2}{\partial x}+\frac{\partial\bar{w}_2}{\partial z}=0. \quad (18)$$

Case 1 For Anisotropic permeability

Solving equation (11) under the slip boundary conditions given by Sparrow *et. al.*[12] and modified by Shah and Bhat[13] with the addition of slider velocity U to[12]

$$u=\frac{1}{s_1}\frac{\partial u}{\partial z}+U \text{ when } z=0\ ;\ u=-\frac{1}{s_2}\frac{\partial u}{\partial z} \text{ when } z=h, \quad (19)$$

where

$$\frac{1}{s_1}=\frac{\sqrt{\varphi_x\eta_x}}{5},\ \frac{1}{s_2}=\frac{\sqrt{\psi_x m_x}}{5};\ \frac{1}{s_i}\ (i=1,2),$$

being slip parameter ; η_x, m_x are porosities in the x-direction for lower and upper porous regions respectively, one obtain

$$u=\frac{1}{\eta}\left[\frac{z^2}{2}-\frac{s_1s_2hz}{s}\left(\frac{h}{2}+\frac{1}{s_2}\right)-\frac{hs_2}{s}\left(\frac{h}{2}+\frac{1}{s_2}\right)\right]\frac{\partial}{\partial x}\left(p-\frac{1}{2}\mu_0\bar{\mu}H^2\right)+\frac{s_1s_2}{s}\left[\left(\frac{1}{s_2}+h\right)-z\right]U, \quad (20)$$

where

$$s=s_1+s_2+hs_1s_2\ .$$

Substituting the above value of u in the integral form of continuity equation (12), yields

$$\frac{\partial}{\partial x}\left[\frac{1}{\eta}\left\{\frac{h^3}{6}-\frac{s_1s_2h^3}{2s}\left(\frac{h}{2}+\frac{1}{s_2}\right)-\frac{s_2h^2}{s}\left(\frac{h}{2}+\frac{1}{s_2}\right)\right\}\frac{\partial}{\partial x}\left(p-\frac{1}{2}\mu_0\bar{\mu}H^2\right)+\frac{s_1s_2hU}{s}\left(\frac{1}{s_2}+\frac{h}{2}\right)\right]+w_h-w_0=0. \quad (21)$$

Substituting equations (13) and (14) in the continuity equation for upper porous region (17), and integrating with respect to z across the upper porous matrix ($h, h+l_1$), yields

$$\frac{\psi_z}{\eta}\frac{\partial}{\partial z}\left(P-\frac{1}{2}\mu_0\bar{\mu}H^2\right)\bigg|_{z=h}=\frac{\psi_x}{\eta}\frac{\partial^2}{\partial x^2}\left(p-\frac{1}{2}\mu_0\bar{\mu}H^2\right)l_1, \quad (22)$$

using Morgan-Cameron approximation[10] and the fact that surface $z=h+l_1$ is non-porous.

Substituting equations (15) and (16) in the continuity equation for lower porous region (18) and integrating with respect to z across the lower porous matrix ($-l_2, 0$), yields

$$\frac{\varphi_z}{\eta}\frac{\partial}{\partial z}\left(P-\frac{1}{2}\mu_0\bar{\mu}H^2\right)\bigg|_{z=0}=-\frac{\varphi_x}{\eta}\frac{\partial^2}{\partial x^2}\left(p-\frac{1}{2}\mu_0\bar{\mu}H^2\right)l_2, \quad (23)$$

using Morgan-Cameron approximation[10] and the fact that surface $z=-l_2$ is non-porous.

Considering the normal component of velocity across the film-porous interface are continuous, so that $w_h=w\big|_{z=h}=\dot{h}+\overline{w_1},\ w_0=w\big|_{z=0}=\overline{w_2}$, using equations (14),(16),(21) and (22)-(23), one obtain

$$\frac{\partial}{\partial x}\left[g\frac{\partial}{\partial x}\left(p-\frac{1}{2}\mu_0\bar{\mu}H^2\right)\right]=\frac{\partial f}{\partial x}, \quad (24)$$

where

$$g=\frac{1}{12\eta s}[h^2(12+4hs_1+4hs_2+h^2s_1s_2)+12s\,(\psi_xl_1+\varphi_xl_2)],$$

$$f=\frac{s_1Uh}{2s}(2+hs_2)+x\dot{h},$$

which is known as Reynolds's type equation for the considered phenomenon.

As mentioned earlier, here magnetic field is considered to be oblique to the lower plate and vanishing at the inlet and outlet of the bearing as

$$H^2=K\,x\,(A-x), \quad (25)$$

where K being a quantity chosen to suit the dimensions of both sides of equation (25).

Introducing the dimensionless quantities

$$X=\frac{x}{A},\ \bar{h}=\frac{h}{h_1},\ \overline{\psi_j}=\frac{\psi_j}{h_1^2},$$

$$\overline{\varphi_j}=\frac{\varphi_j}{h_1^2},\ \bar{l_i}=\frac{l_i}{h_1},\ \overline{s_1}=s_1h_1,\ \overline{s_2}=s_2h_1,$$

$$a=\frac{h_2}{h_1},\bar{\delta}=\frac{\delta}{h_1},$$

$$\bar{p}=\frac{h_1^2p}{\eta AU},\ \mu^*=\frac{\mu_0\bar{\mu}KAh_1^2}{\eta U},$$

$$S=\frac{-2\dot{h}A}{Uh_1};\ i=1,2;\ j=x,z.$$

Then the dimensionless form of equations (1)-(5) and (24)-(25) becomes

$$\bar{h_i}=a-(a-1)X\,;0\le X\le 1$$

$$\bar{h_e}=a\exp(-X\ln a)\,;0\le X\le 1$$

$$\bar{h_s}=\sec\left\{\frac{\pi}{2}(1-X)\right\};0<X\le 1$$

$$\bar{h_c}=4\bar{\delta}X^2-(a-1+4\bar{\delta})X+a\,;0\le X\le 1$$

$$\bar{h_p}=1\,;0\le X\le 1$$

and

$$\frac{d}{dX}\left[G\frac{d}{dX}\left\{\bar{p}-\frac{1}{2}\mu^*X(1-X)\right\}\right]=\frac{dE}{dX}, \quad (26)$$

where

$$G=\bar{h}^2(12+4\bar{h}\,\overline{s_1}+4\bar{h}\,\overline{s_2}+\bar{h}^2\,\overline{s_1}\,\overline{s_2})+12\bar{s}(\overline{\psi_x}\bar{l_1}+\overline{\varphi_x}\bar{l_2}), \quad (27)$$

$$E=-6S\bar{s}X+6\overline{s_1}\,\bar{h}\,(2+\bar{h}\,\overline{s_2}). \quad (28)$$

Also,

$$H^2=KA^2X(1-X). \quad (29)$$

Equation (26) with (27)-(28) is known as dimensionless form of Reynolds's equation for anisotropic permeable porous plate with respect to both upper and lower porous matrix.

Case 2 For Isotropic permeability

In this case $\phi_x = \phi_z = \psi_x = \psi_z$.

By following similar procedure as in Case 1, the following dimensionless form of Reynolds's equation for isotropic permeable porous plate with respect to both upper and lower porous matrix is obtained.

$$\frac{d}{dX}\left[G\frac{d}{dX}\left\{\bar{p}-\frac{1}{2}\mu^* X(1-X)\right\}\right]=\frac{dE}{dX}, \quad (30)$$

where

$$G=\bar{h}^2(12+4\bar{h}\,\bar{s}_1+4\bar{h}\,\bar{s}_2+\bar{h}^2\bar{s}_1\,\bar{s}_2)+12\bar{s}\,\bar{\varphi}_x(\bar{l}_1+\bar{l}_2), \quad (31)$$

$$E=-6S\bar{s}X+6\bar{s}_1\,\bar{h}\,(2+\bar{h}\,\bar{s}_2). \quad (32)$$

Equation (30) with (31)-(32) is known as dimensionless form of Reynolds's equation for isotropic permeable porous plate with respect to both upper and lower porous matrix.

3. Calculation of Dimensionless Load Carrying Capacity

Since the pressure is negligible on the boundaries of the slider bearing compared to inside pressure, solving equation (26) under boundary conditions

$$\bar{p}=0 \text{ when } X=0,1;$$

the dimensionless film pressure $\bar{p}$ is obtained as follows:

$$\bar{p}=\frac{1}{2}\mu^* X(1-X)+\int_0^X \frac{E-Q}{G}dX,$$

where

$$Q=\frac{\int_0^1 \frac{E}{G}dX}{\int_0^1 \frac{1}{G}dX}.$$

The load carrying capacity W is expressed in dimensionless form as

$$\bar{W}=\frac{h_1^2 W}{\eta A^2 BU}=\frac{\mu^*}{12}-\int_0^1 X\left(\frac{E-Q}{G}\right)dX,$$

where

$$W=\int_0^B\int_0^A p\;dxdy.$$

For anisotropic case G, E are given by equations (27)-(28), and for isotropic case G, E are given by equations (31)-(32).

4. Calculation of Results

The dimensionless load carrying capacity ($\bar{W}$) for various designed slider bearings (that is, slider bearings having inclined pad stator, exponential pad stator, secant pad stator, convex pad stator, parallel pad stator) are calculated for various sizes of upper and lower porous matrix using Simpson's one third rule with step size 0.1, considering following values of the parameters :

$$\eta_x = 0.64,\; m_x = 0.81,\; \mu_0 = 4\pi\times10^{-7}\,(kgms^{-2}A^{-2}),$$

$$\bar{\mu}=0.05,\; K=10^9\,(A^2m^{-4}),$$

$$A=0.15\,(m),\;\; \eta=0.012\,(kgm^{-1}s^{-1}),\; U=1.0\,(ms^{-1}),$$

$$\dot{h}=-0.005\;(ms^{-1}),\; a=2.0\,(m),$$

$$\bar{\delta}=0.3.$$

In the following cases, the notations used are

$\bar{W}_i$ - Dimensionless load carrying capacity for slider bearing having inclined pad stator

$\bar{W}_e$ - Dimensionless load carrying capacity for slider bearing having exponential pad stator

$\bar{W}_S$ - Dimensionless load carrying capacity for slider bearing having secant pad stator

$\bar{W}_c$ - Dimensionless load carrying capacity for slider bearing having convex pad stator

$\bar{W}_p$ - Dimensionless load carrying capacity for slider bearing having parallel pad stator

Case 1 For Anisotropic permeability

Table 1. Values of $\bar{W}$ for φ_x=0.001, ψ_x=0.00001

Dimensionless load carrying capacity $\bar{W}$	$\bar{l}_1=0, \bar{l}_2=0$	% increase in $\bar{W}$ w.r.t. $\bar{W}_p$
$\bar{W}_i$	0.3979	127.24
$\bar{W}_e$	0.3998	128.33
$\bar{W}_s$	0.3245	85.32
$\bar{W}_c$	0.4078	132.90
$\bar{W}_p$	0.1751	-

Table 2. Values of $\overline{W}$ for φ_x=0.001, ψ_x=0.00001

Dimensionless load carrying capacity $\overline{W}$	$\overline{l_1}=1, \overline{l_2}=1$	% increase in $\overline{W}$ w.r.t. $\overline{W_p}$
$\overline{W_i}$	0.2648	59.42
$\overline{W_e}$	0.2637	58.76
$\overline{W_s}$	0.2476	49.07
$\overline{W_c}$	0.2626	58.10
$\overline{W_p}$	0.1661	-

Table 3. Values of $\overline{W}$ for φ_x=0.001, ψ_x=0.00001

Dimensionless load carrying capacity $\overline{W}$	$\overline{l_1}=1, \overline{l_2}=5$	% increase in $\overline{W}$ w.r.t. $\overline{W_p}$
$\overline{W_i}$	0.1968	19.78
$\overline{W_e}$	0.1961	19.35
$\overline{W_s}$	0.2030	23.55
$\overline{W_c}$	0.1953	18.87
$\overline{W_p}$	0.1643	-

Table 4. Values of $\overline{W}$ for φ_x=0.001, ψ_x=0.00001

Dimensionless load carrying capacity $\overline{W}$	$\overline{l_1}=5, \overline{l_2}=1$	% increase in $\overline{W}$ w.r.t. $\overline{W_p}$
$\overline{W_i}$	0.2627	58.25
$\overline{W_e}$	0.2616	57.59
$\overline{W_s}$	0.2464	48.43
$\overline{W_c}$	0.2605	56.93
$\overline{W_p}$	0.1660	-

Table 5. Values of $\overline{W}$ for φ_x=0.00001, ψ_x=0.001

Dimensionless load carrying capacity $\overline{W}$	$\overline{l_1}=0, \overline{l_2}=0$	% increase in $\overline{W}$ w.r.t. $\overline{W_p}$
$\overline{W_i}$	0.4089	133.92
$\overline{W_e}$	0.4111	135.18
$\overline{W_s}$	0.3320	89.93
$\overline{W_c}$	0.4206	140.62
$\overline{W_p}$	0.1748	-

Table 6. Values of $\overline{W}$ for φ_x=0.00001, ψ_x=0.001

Dimensionless load carrying capacity $\overline{W}$	$\overline{l_1}=1, \overline{l_2}=1$	% increase in $\overline{W}$ w.r.t. $\overline{W_p}$
$\overline{W_i}$	0.2703	62.73
$\overline{W_e}$	0.2693	62.13
$\overline{W_s}$	0.2517	51.54
$\overline{W_c}$	0.2686	61.71
$\overline{W_p}$	0.1661	-

Table 7. Values of $\overline{W}$ for φ_x=0.00001, ψ_x=0.001

Dimensionless load carrying capacity $\overline{W}$	$\overline{l_1}=1, \overline{l_2}=5$	% increase in $\overline{W}$ w.r.t. $\overline{W_p}$
$\overline{W_i}$	0.2681	61.51
$\overline{W_e}$	0.2671	60.90
$\overline{W_s}$	0.2504	50.84
$\overline{W_c}$	0.2663	60.42
$\overline{W_p}$	0.1660	-

Table 8. Values of $\overline{W}$ for φ_x=0.00001, ψ_x=0.001

Dimensionless load carrying capacity $\overline{W}$	$\overline{l_1}=5, \overline{l_2}=1$	% increase in $\overline{W}$ w.r.t. $\overline{W_p}$
$\overline{W_i}$	0.1987	20.94
$\overline{W_e}$	0.1981	20.57
$\overline{W_s}$	0.2048	24.65
$\overline{W_c}$	0.1973	20.09
$\overline{W_p}$	0.1643	-

Case 2 For Isotropic permeability

Table 9. Values of $\overline{W}$ for φ_x=0.000001, ψ_x=0.000001

Dimensionless load carrying capacity $\overline{W}$	$\overline{l_1}=5, \overline{l_2}=5$	% increase in $\overline{W}$ w.r.t. $\overline{W_p}$
$\overline{W_i}$	0.4582	157.85
$\overline{W_e}$	0.4612	159.54
$\overline{W_s}$	0.3610	103.15
$\overline{W_c}$	0.4730	166.18
$\overline{W_p}$	0.1777	-

Table 10. Values of $\overline{W}$ for φ_x=0.000001, ψ_x=0.000001

Dimensionless load carrying capacity $\overline{W}$	$\overline{l_1}=5, \overline{l_2}=10$	% increase in $\overline{W}$ w.r.t. $\overline{W_p}$
$\overline{W_i}$	0.4555	156.76
$\overline{W_e}$	0.4585	158.46
$\overline{W_s}$	0.3594	102.59
$\overline{W_c}$	0.4699	164.88
$\overline{W_p}$	0.1774	-

Table 11. Values of $\overline{W}$ for φ_x=0.000001, ψ_x=0.000001

Dimensionless load carrying capacity $\overline{W}$	$\overline{l_1}=10, \overline{l_2}=5$	% increase in $\overline{W}$ w.r.t. $\overline{W_p}$
$\overline{W_i}$	0.4555	156.76
$\overline{W_e}$	0.4585	158.46
$\overline{W_s}$	0.3594	102.59
$\overline{W_c}$	0.4699	164.88
$\overline{W_p}$	0.1774	-

Table 12. Values of $\overline{W}$ for φ_x=0.00001, ψ_x=0.00001

Dimensionless load carrying capacity $\overline{W}$	$\overline{l_1}=5, \overline{l_2}=5$	% increase in $\overline{W}$ w.r.t. $\overline{W_p}$
$\overline{W_i}$	0.4109	136.97
$\overline{W_e}$	0.4123	137.77
$\overline{W_s}$	0.3331	92.10
$\overline{W_c}$	0.4186	141.41
$\overline{W_p}$	0.1734	-

Table 13. Values of $\overline{W}$ for φ_x=0.00001, ψ_x=0.00001

Dimensionless load carrying capacity $\overline{W}$	$\overline{l_1}=5, \overline{l_2}=10$	% increase in $\overline{W}$ w.r.t. $\overline{W_p}$
$\overline{W_i}$	0.3947	129.34
$\overline{W_e}$	0.3955	129.81
$\overline{W_s}$	0.3238	88.15
$\overline{W_c}$	0.4002	132.54
$\overline{W_p}$	0.1721	-

Table 14. Values of $\overline{W}$ for φ_x=0.00001, ψ_x=0.00001

Dimensionless load carrying capacity $\overline{W}$	$\overline{l_1}=10, \overline{l_2}=5$	% increase in $\overline{W}$ w.r.t. $\overline{W_p}$
$\overline{W_i}$	0.3947	129.34
$\overline{W_e}$	0.3955	129.81
$\overline{W_s}$	0.3238	88.15
$\overline{W_c}$	0.4002	132.54
$\overline{W_p}$	0.1721	-

5. Discussion of Results

The mathematical study of water based magnetic fluid lubricated various designed slider bearing are discussed and compared for dimensionless load carrying capacity $\overline{W}$ with slider bearing having parallel pad stator considering effects of porosity, slip velocity at both the ends, and squeeze velocity under an oblique magnetic field. The two cases of anisotropic permeability and isotropic permeability with respect to both upper and lower porous matrix are discussed for various sizes porous matrixes attached at both the plates. The following observations can be made from the results:

(1) It is observed form tables 1-4 that maximum $\overline{W}$ is obtained when $\overline{l_1}$ = 0 and $\overline{l_2}$ = 0. But with the insertation of porous layer at both the plates, maximum $\overline{W}$ can be obtained when $\overline{l_1}$ = 1 and $\overline{l_2}$ = 1. The almost same behaviour is obtained when $\overline{l_1}$ = 5 and $\overline{l_2}$ = 1; that is, when the porous layer attached to the upper plate (stator) is thick and porous layer attached to the lower plate (slider) is thin. But if we reverse the thickness of the porous plates; that is, when $\overline{l_1}$ = 1 and $\overline{l_2}$ = 5 then the increase of $\overline{W}$ is substantially less. Moreover, the percentage increases in $\overline{W}$ for various slider bearings with respect to slider bearing with parallel plate stator are as shown in tables.

(2) It is observed form tables 5-8 that maximum $\overline{W}$ is obtained when $\overline{l_1}=0$ and $\overline{l_2}=0$. But with the insertation of porous layer at both the plates, maximum $\overline{W}$ can be obtained when $\overline{l_1}$ = 1 and $\overline{l_2}$ = 1. The almost same behaviour is obtained when $\overline{l_1}$ = 1 and $\overline{l_2}$ = 5; that is, when the porous layer attached to the lower plate (slider) is thick and porous layer attached to the upper plate (stator) is thin. But if we reverse the thickness of the porous plates; that is, when $\overline{l_1}$ = 5 and $\overline{l_2}$ = 1 then the increase of $\overline{W}$ is substantially less. Moreover, the percentage increases in $\overline{W}$ for various slider bearings with respect to slider bearing with parallel plate stator are as shown in tables.

In summary, when the permeability of the upper porous layer is small as compared to lower porous layer, then $\overline{W}$ increases with the increase of thickness of upper porous layer. Similarly, when the permeability of the lower porous layer is small as compared to upper porous layer, then $\overline{W}$ increases with the increase of thickness of lower porous layer.

Thus, maximum $\overline{W}$ can be obtained when permeability decreases and thickness of the porous layer increases.

It is observed form tables 9-11 that maximum $\overline{W}$ is obtained when $\overline{l_1}=5$ and $\overline{l_2}=5$. Also, $\overline{W}$ remains same whether $\overline{l_1}$ = 5 and $\overline{l_2}$ = 10 or $\overline{l_1}$ = 10 and $\overline{l_2}$ = 5. Similar type of behaviour for $\overline{W}$ is obtained for tables 12-14. Moreover, for smaller values of permeabilities φ_x and ψ_x, better $\overline{W}$ is obtained (refer tables 9-11) as compared to larger values (refer tables 12-14).

The following table 15 indicates the comparison of $\overline{W}$ for various bearings.

Table 15. Comparison of dimensionless load carrying capacity for various bearings

	Values of $\bar{l}_1$	Values of $\bar{l}_2$	Comparison of $\overline{W}$ for various bearings
For Table 1	0	0	$\overline{W_c} > \overline{W_e} > \overline{W_i} > \overline{W_s} > \overline{W_p}$
For Table 2	1	1	$\overline{W_i} > \overline{W_e} > \overline{W_c} > \overline{W_s} > \overline{W_p}$
For Table 3	1	5	$\overline{W_s} > \overline{W_i} > \overline{W_e} > \overline{W_c} > \overline{W_p}$
For Table 4	5	1	$\overline{W_i} > \overline{W_e} > \overline{W_c} > \overline{W_s} > \overline{W_p}$
For Table 5	0	0	$\overline{W_c} > \overline{W_e} > \overline{W_i} > \overline{W_s} > \overline{W_p}$
For Table 6	1	1	$\overline{W_i} > \overline{W_e} > \overline{W_c} > \overline{W_s} > \overline{W_p}$
For Table 7	1	5	$\overline{W_i} > \overline{W_e} > \overline{W_c} > \overline{W_s} > \overline{W_p}$
For Table 8	5	1	$\overline{W_s} > \overline{W_i} > \overline{W_e} > \overline{W_c} > \overline{W_p}$
For Table 9	5	5	$\overline{W_c} > \overline{W_e} > \overline{W_i} > \overline{W_s} > \overline{W_p}$
For Table 10	5	10	$\overline{W_c} > \overline{W_e} > \overline{W_i} > \overline{W_s} > \overline{W_p}$
For Table 11	10	5	$\overline{W_c} > \overline{W_e} > \overline{W_i} > \overline{W_s} > \overline{W_p}$
For Table 12	5	5	$\overline{W_c} > \overline{W_e} > \overline{W_i} > \overline{W_s} > \overline{W_p}$
For Table 13	5	10	$\overline{W_c} > \overline{W_e} > \overline{W_i} > \overline{W_s} > \overline{W_p}$
For Table 14	10	5	$\overline{W_c} > \overline{W_e} > \overline{W_i} > \overline{W_s} > \overline{W_p}$

6. Conclusions

Based upon the above formulation, and results & discussion the following conclusions can be drawn for designing slider bearing:

(1) Because of having the self lubrication property of the porous plate bearing, it is suggested to have both the porous plate bearing for better self lubrication.

(2) When the permeability of the upper porous layer is small as compared to lower porous layer, then $\overline{W}$ increases with the increase of thickness of upper porous layer. Similarly, when the permeability of the lower porous layer is small as compared to upper porous layer, then $\overline{W}$ increases with the increase of thickness of lower porous layer.

(3) For isotropic case more better $\overline{W}$ is obtained.

(4) It should be noted that a constant magnetic field does not enhance $\overline{W}$ in this model since $\partial H / \partial x = 0$ in equation (11).

(5) It is observed form table 15 that the suggestive design of bearing is either inclined or convex pad stator surfaces and occasionally secant pad stator surface.

REFERENCES

[1] Rosensweig R E. Ferrohydrodynamics. New York: Cambridge University Press;1985.

[2] Mehta R V, Upadhyay R V. Science and Technology of ferrofluids. Current Science 1999; 76: 305-312.

[3] Tipei N. Theory of Lubrication with Ferrofluids: Application to short bearings. Transactions of ASME 1982; 104: 510-515.

[4] Agrawal V K. Magnetic fluid based porous inclined slider bearing. Wear 1986; 107: 133-139.

[5] Sinha P, Chandra P, Kumar D. Ferrofluid lubrication of cylindrical rollers with cavitation. Acta Mechanica 1993; 98: 27-38.

[6] Ram P and Verma P D S. Ferrofluid lubrication in porous inclined slider bearing. Indian Journal of Pure & Applied Mathematics 1999; 30(12): 1273-1281.

[7] Shah R C, Bhat M V. Ferrofluid lubrication in porous slider bearing with velocity slip. International Journal of Mechanical Sciences 2002; 44: 2495-2502.

[8] Shah R C, Bhat M V. Ferrofluid squeeze film between curved annular plates including rotation of magnetic particles. Journal of Engineering Mathematics 2005; 51: 317-324.

[9] Ahmad N and Singh JP. Magnetic fluid lubrication of porous-pivoted slider bearing with slip velocity. Journal of Engineering Tribology 2007; 221: 609-613.

[10] Shah R C, Patel D B. Mathematical Modeling of newly designed Ferrofluid Based Slider Bearing Including Effects of Porosity, Anisotropic Permeability, Slip Velocity at Both the Ends, and Squeeze Velocity. Applied Mathematics 2012; 2(5): 176-183.

[11] Shah R C, Bhat M V. Analysis of a porous exponential slider bearing lubricated with a ferrofluid considering slip velocity. Journal of the Brazilian Society of Mechanical Sciences and Engineering 2003; 25(3) : 264-267.

[12] Sparrow E M, Beavers G S, Hwang I T. Effect of velocity slip on porous walled squeeze films. Journal of Lubrication Technology 1972; 94: 260-265.

[13] Shah R C, Bhat M V. Ferrofluid lubrication equation for porous bearing considering anisotropic permeability and slip velocity. Indian Journal of Engineering & Material Sciences 2003; 10 : 277-281.